Electronic Supplementary Information

Oleylamine Passivated Hydrophobic Sulfur Quantum Dots as Highly Efficient Adsorbents for Gaseous Iodine Sequestration

Hammad Hasan, Neelima Varshney and Md Palashuddin Sk*

Nanoscale Functional Materials Laboratory, Department of Chemistry, Aligarh Muslim University, Aligarh-202002, Uttar Pradesh, India

E-mail: palashuddin.ch@amu.ac.in

Experimental Section

Materials

All chemicals and reagents were purchased from commercial suppliers and used as received without further purification.

Synthesis of Sdots

Sdots were synthesized through a solvothermal approach using elemental sulfur and oleylamine. Briefly, elemental sulfur (240 mg, 7.5 mmol) was added to oleylamine (5 mL) and stirred at 50 °C for 5 min, during which the reaction mixture gradually changed to an orange color. The resulting mixture was then transferred into a Teflon-lined autoclave and heated at 180 °C for 4 h. After naturally cooling to room temperature, a dark yellow-brown viscous liquid product was obtained.

The synthesized Sdots exhibited hydrophobic behavior, being readily dispersible in n-hexane while remaining immiscible with water and ethanol. For purification, the crude product was dissolved in n-hexane followed by the addition of ethanol (5 mL). The mixture was subsequently centrifuged to remove unreacted species and excess organic residues, after which the ethanol layer was discarded. The purified Sdots dispersed in n-hexane were collected for further characterization and adsorption studies.

Preparation of Sdots-coated Cotton for Contact Angle Measurement

For contact angle measurements, 200 mg of medicated cotton was immersed in 2 mL of an Sdots dispersion in n-hexane (20 mg mL^{-1}) and dried at room temperature. The coating process was repeated three times to ensure uniform deposition of Sdots over the cotton surface. The dried Sdots-coated cotton was subsequently used for contact angle analysis.

Iodine Vapor Adsorption Study

The iodine vapor adsorption performance of the synthesized Sdots was evaluated by exposing the material to iodine vapor generated from solid iodine crystals. Briefly, iodine crystals were placed in a broad open beaker inside a sealed 1000 mL oil bath setup, while a watch glass containing 100 mg of Sdots was positioned alongside the iodine source. The system was tightly sealed using aluminium foil to minimize vapor loss, and an excess amount of iodine was used to ensure saturated iodine vapor conditions throughout the experiment. The adsorption setup was maintained at 75 °C for 6 h, and the adsorption behavior was monitored at regular 2 h intervals. Following exposure, the watch glass containing the Sdots was weighed, and the amount of adsorbed iodine was calculated from the corresponding weight gain. A distinct color change of the Sdots from brown to black was observed after iodine exposure, indicating efficient adsorption of iodine vapor. The iodine uptake capacity was calculated using the following equation:

$$q_t = \frac{W_t - W_0}{W_0} \times 100$$

Where W_0 and W_t represent the initial and final masses of the Sdots, respectively.

Iodine Vapor Adsorption under Humid Conditions

The iodine vapor adsorption experiment under humid conditions was performed following the same procedure described above, except that an open 5 mL glass vial containing distilled water was additionally placed inside the sealed adsorption setup to generate a humid atmosphere. Under these conditions, the synthesized Sdots exhibited an iodine adsorption capacity of 2307 mg g^{-1}.

Adsorption kinetics Study

The adsorption kinetics of iodine vapor uptake by Sdots was further analyzed using the Ho and McKay pseudo-second-order kinetic model according to the following equation:

$$\frac{t}{q_t} = \frac{1}{k_2 {q_e}^2} + \frac{t}{q_e}$$

where q_t and q_e represent the amounts of iodine adsorbed (mg g^{-1}) at time t and at equilibrium, respectively, while k_2 denotes the pseudo-second-order rate constant. The adsorption data exhibited a good linear fit with an R^2 value of 0.964, indicating efficient iodine uptake governed by the strong affinity of iodine molecules toward the hydrophobic Sdots surface.

Adsorption of Iodine from Cyclohexane Solution

Liquid-phase iodine adsorption experiments were carried out using iodine dissolved in cyclohexane. Briefly, 5 mg of Sdots was added to 3 mL of a 2 mM iodine solution in cyclohexane under ambient conditions. UV-vis absorption spectra of the solution were recorded at different time intervals (0, 4, 8, 12, 16, 20, and 24 min) to monitor the decrease in the characteristic iodine absorption band at ~522 nm.

The adsorption capacity of Sdots toward molecular iodine and the corresponding removal efficiency were determined using the following equations:

$$W = \frac{(C_0 - C_t)V}{m}$$

$$Q(\%) = \frac{(C_0 - C_t) \times 100}{C_0}$$

Where W represents the equilibrium adsorption capacity (mg g^{-1}), while C_0 and C_t denote the initial and residual concentrations of iodine in solution (mg L^{-1}), respectively. V (L) corresponds to the volume of the iodine solution, and m (g) is the mass of Sdots used for adsorption.

Regeneration and Recyclability Studies

To evaluate the practical applicability and recyclability of the Sdots, successive adsorption–desorption cycles were performed. The iodine-loaded Sdots were immersed in methanol, where spontaneous desorption occurred. The methanol phase gradually turned from colorless to dark brown, confirming effective release of adsorbed iodine species. After 6 h of standing, the regenerated Sdots recovered their dark original brown colour, indicating successful regeneration of the material.

Elemental Composition and Molar Ratio Calculations for Sdots

To quantify the elemental composition of the synthesized Sdots and correlate it with iodine adsorption performance, CHNS elemental analysis and quantitative XPS measurements were performed. The CHNS results are summarized below.

Elements	Carbon (C)	Hydrogen (H)	Nitrogen (N)	Sulfur (S)
Weight (%)	77.99	12.4	4.02	1.6

The bulk analysis reveals the sulfur content of 1.6 wt%, while quantitative XPS analysis indicates a surface sulfur content of 1.3 at%, corresponding to approximately 3.37 wt%. A comparison of bulk and surface sulfur contents shows a clear enrichment at the surface, with a surface-to-bulk mass ratio of approximately 3.37:1.6 ≈ 2.1:1, indicating the enrichment of sulfur species on the surface of the Sdots.

Control Experiments

Control experiments were carried out under identical iodine vapor adsorption conditions using 100 mg of elemental sulfur powder and 100 mg of oleylamine separately in place of Sdots. The iodine uptake was determined from the corresponding weight gain after 6 h of exposure at 75 °C. Oleylamine exhibited an iodine uptake capacity of 1260.9 mg g^{-1}, while elemental sulfur showed an uptake capacity of 683.6 mg g^{-1}.

Iodine uptake capacity of Sdots= 2.676 g g^{-1}

$$Moles\ of\ Iodine\ adsorbed = 2.676/253.8 = 0.0105 mol/g\ Sdots$$

Surface Sulfur to Iodine Molar Ratio

XPS analysis indicates a surface sulfur content of 1.3 at%, corresponding to approximately 3.37 wt%.

3.37g sulfur presents per 100g Sdots, *i.e.* 0.0337g sulfur/g Sdots

$$Moles\ of\ sulfur = \frac{0.0337}{32.06} \cong 0.001\ mole\ /g\ Sdots$$

Surface to Iodine ratio, $0.001: 0.0105 = 0.1: 1$

Surface Nitrogen to Iodine Molar Ratio

Quantitative XPS analysis indicated a nitrogen content of 3.56 at%, corresponding to approximately 4.04 wt%.

4.04g nitrogen presents per 100g Sdots, i.e. 0.0404g nitrogen/g Sdots

$$Moles\ of\ nitrogen = \frac{0.0404}{14.007} \cong 0.003\ mole\ /g\ Sdots$$

Nitrogen to Iodine ratio, $0.003: 0.0105 \cong 0.3: 1$

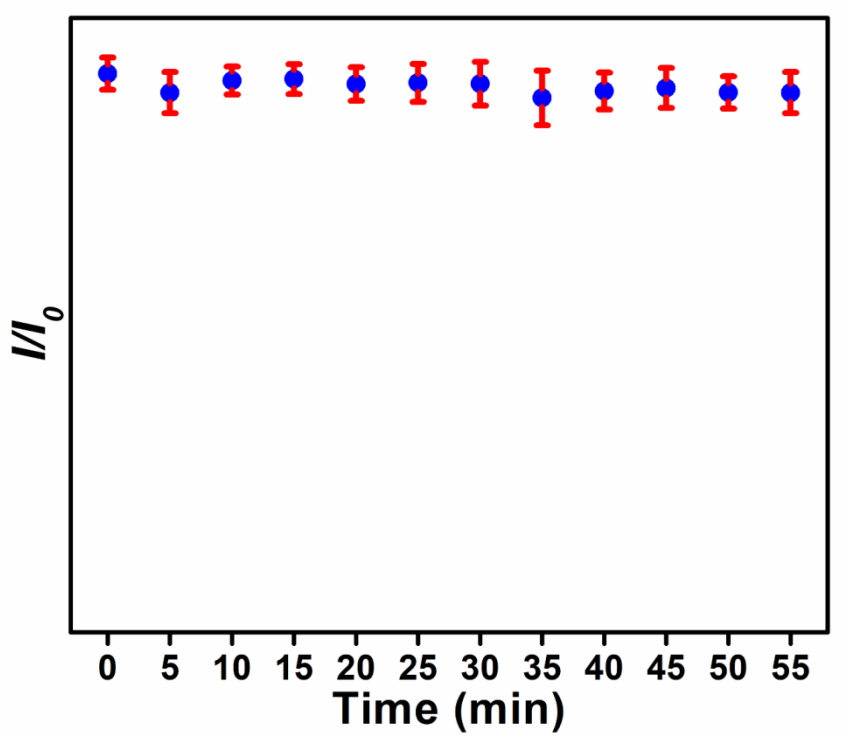

Fig. S1 Photostability plot of Sdots under continuous UV irradiation.

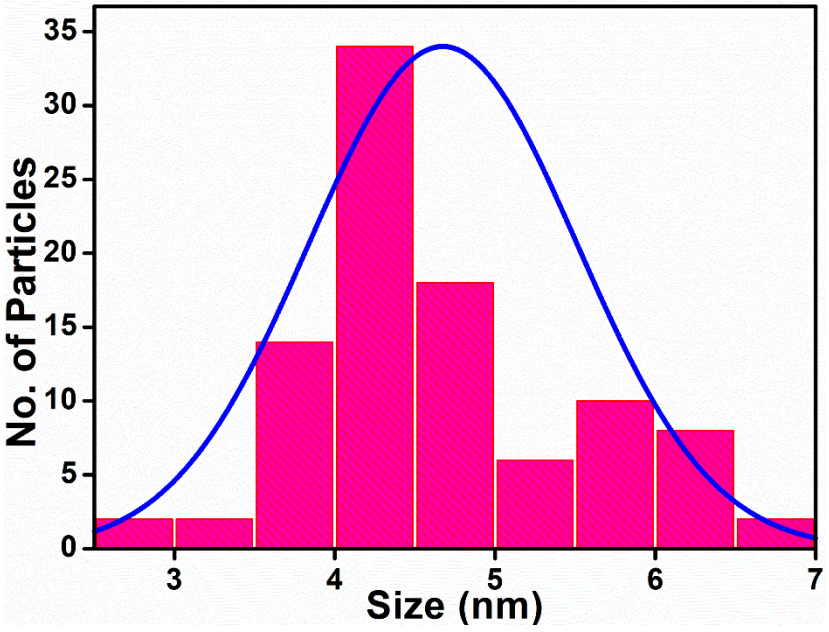

Fig. S2 Particle size distribution histogram of Sdots.

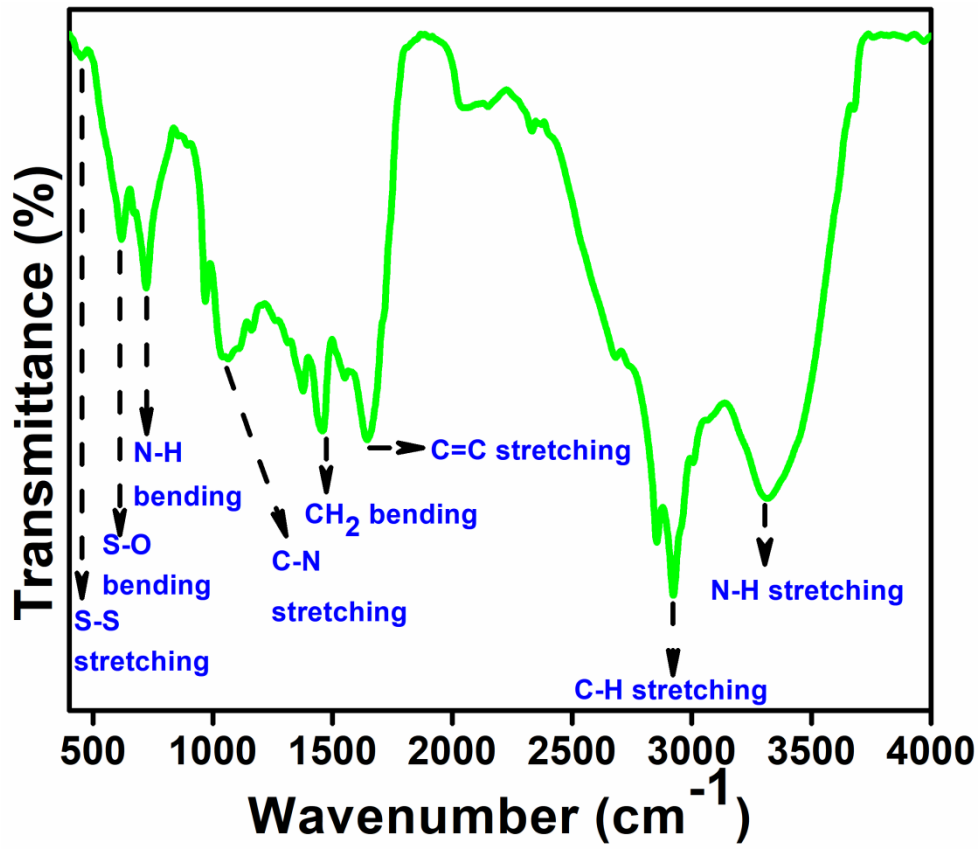

Fig. S3 FTIR spectrum of Sdots showing characteristic surface functional groups.

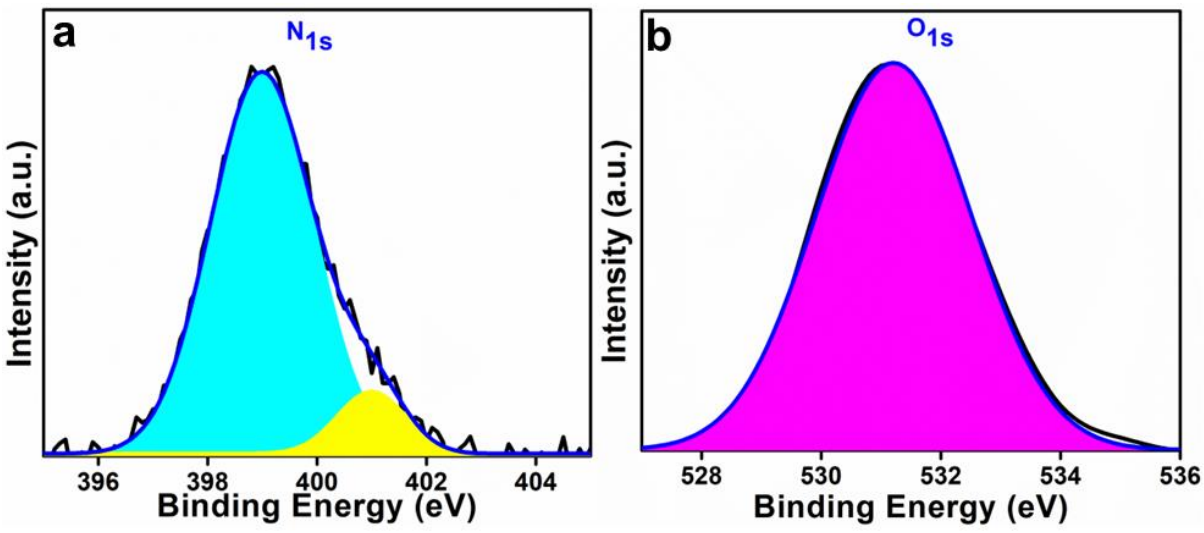

Fig. S4 High-resolution XPS spectra of Sdots consisting of (a) N_{1s} band and (b) O_{1s} band.

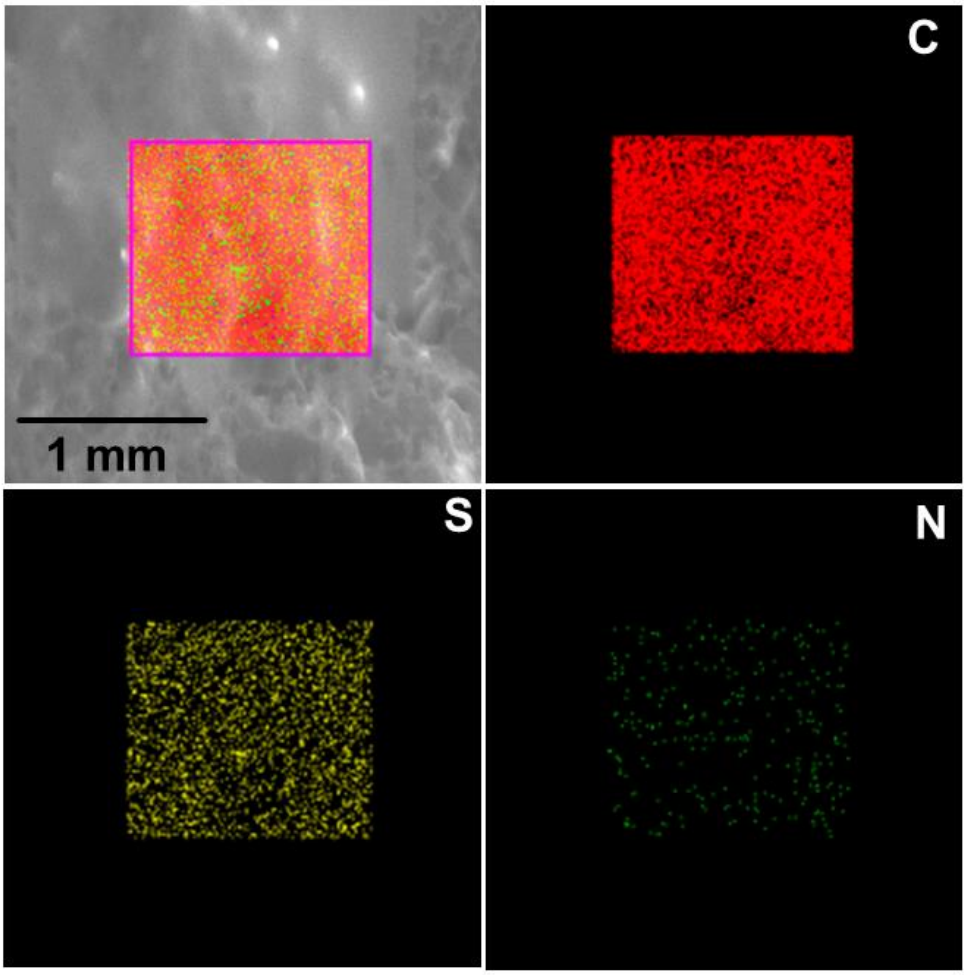

Fig. S5 Elemental mapping of Sdots, indicating the presence of C, S, and N elements.

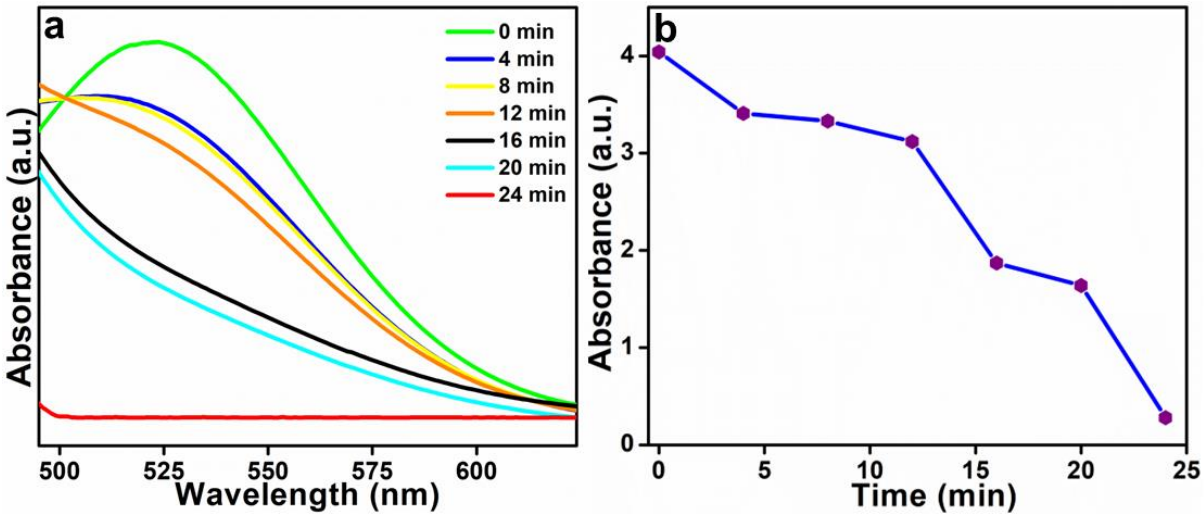

Fig. S6 (a) UV-vis spectra tracking the decrease in iodine concentration in cyclohexane with time. (b) Absorbance at 523 nm decreasing with time.

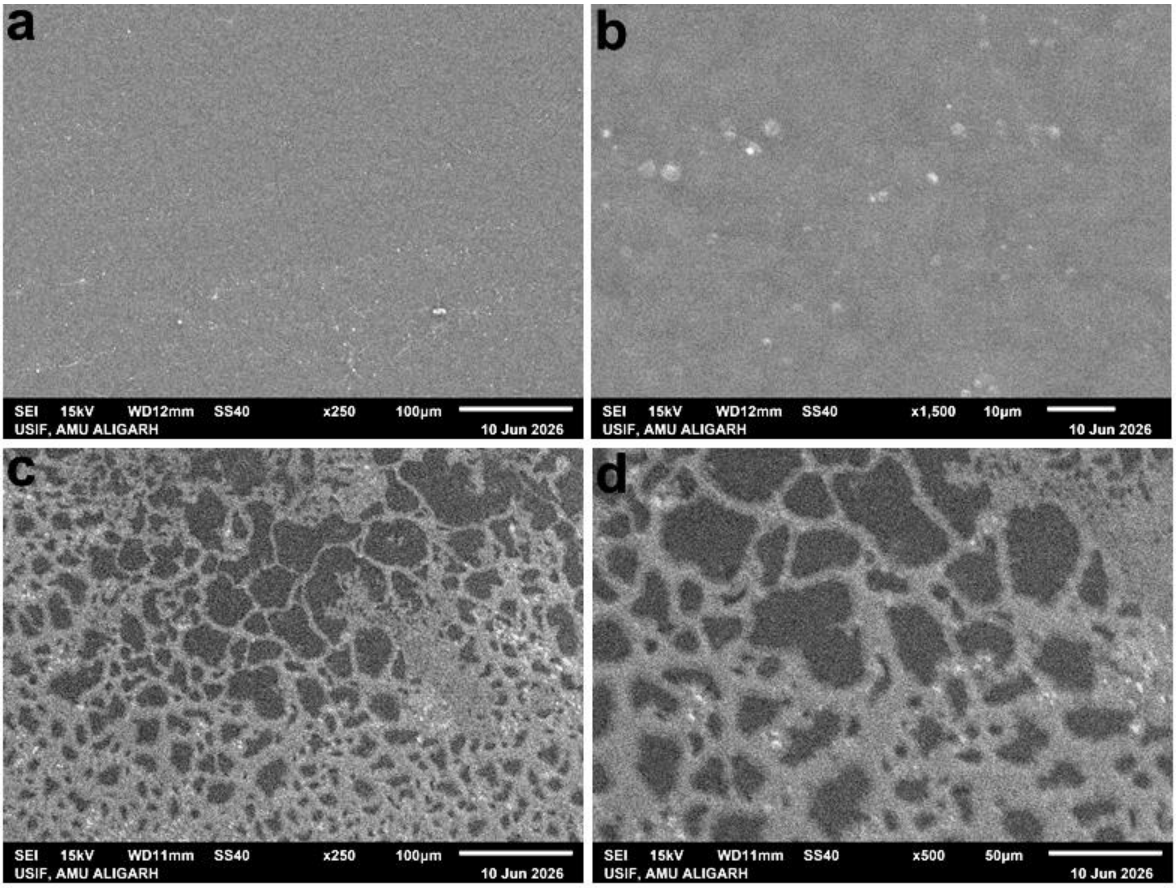

Fig. S7 SEM images of (a & b) pristine Sdots and (c & d) Sdots after iodine adsorption.

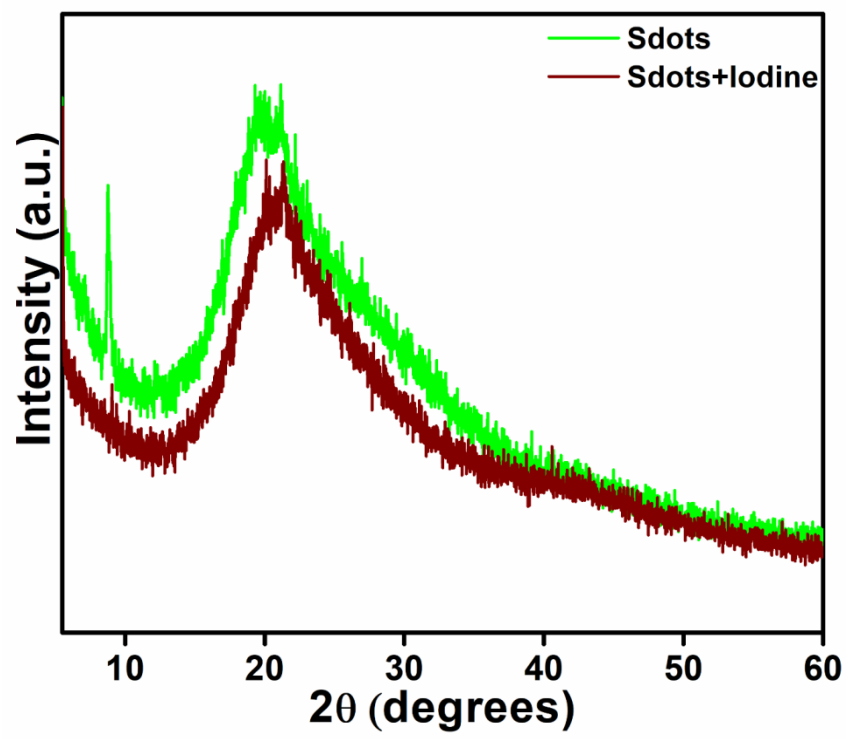

Fig. S8 PXRD patterns of pristine Sdots and iodine-adsorbed Sdots.

Note: The diffraction peak at 2θ = 8.7° in the pristine Sdots arises from interlayer spacing formed in the dried sample.[1]

Reference: 1) *Appl. Sci.* 2024, **14(24)**, 11701.

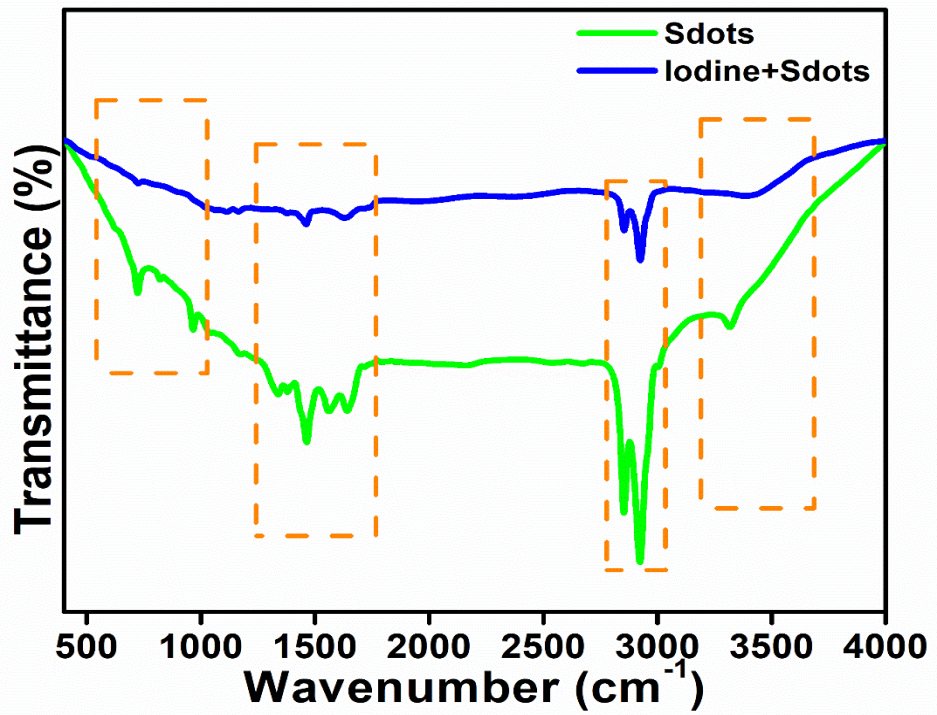

Fig. S9 FTIR spectrum of Sdots and iodine adsorbed Sdots.

Table S1: Comparative overview of iodine adsorption capacities of representative adsorbent materials from recent literature reports.

Material	Class	Synthesis method	Phase	Adsorption capacity (mg/g)	Key remarks	Reference
Bi-Thio HCP	Sulfur-enriched hyper-crosslinked polymer	Friedel-Crafts alkylation of 2,2′-bithiophene	Vapor / aqueous	1960 / 1660	Sulfur-rich porous polymer exhibiting strong iodine affinity through electron-rich sulfur sites; however, the synthesis involves polymerization and prolonged reaction conditions.	RSC Appl. Polym., 2026, DOI: 10.1039/D5LP00400D
CPT-HDI	Cryptand-based polymer	One-step cross-linking reaction (CPT + HDI)	Vapor/ cyclohexane	3520 / 662	The synthesis method is not facile, expensive and requires a long reaction time.	ACS Appl. Polym. Mater. 2026, 8(6), 4092-4102
C4P-Tab	Calix[4]pyrrole POP	Crosslinking of alkynyl calix[4]pyrrole monomers	Vapor / aqueous	3870 / 3960	The material requires a multistep and atom-inefficient synthesis, which increases the cost and limits scalability compared to simpler porous organic polymers.	J. Mater. Chem. A, 2026,14, 13658-13668
CuS/AC	Activated carbon composite	Impregnation	Vapor	486	Non-uniform metal distribution limits adsorption efficiency	Chem. Eng. Sci., 2025, 303, 120955
Cu-CP@CNT	CNT composite	Functionalization + solvothermal	Vapor	729.9	Multistep synthesis and low Adsorption capacity.	J. Water Process Eng., 2025, 69, 106569
Cu-Cu_2O/RGO	Graphene composite	Chemical reduction	Aqueous	152.1	Low adsorption capacity.	J. Environ. Chem. Eng., 2025, 13, 115563
Cdots-Agg	Carbon dot aggregates	Solvothermal (DPT precursor)	Vapor/ aqueous	1007	Mesoporous aggregates enable dual-phase iodine capture but exhibit low	Small, 21(46), 2025, e08118

					adsorption capacity.	
PANI/Bi_2S_3 nanoflowers	Bi_2S_3/polyaniline composite	Chemical oxidative polymerization	Vapor / cyclohexane	3307 / 1306.9	Sulfur-containing composite exhibiting efficient iodine capture through combined Bi-I interactions and nitrogen-containing adsorption sites; however, the material requires inorganic nanocomposite synthesis and polymer incorporation.	Colloids Surf. A Physicochem. Eng. Asp., 2025, 709, 136096
GOF-LS	Graphene organic framework	Multistep	Vapor/ cyclohexane	2320/ 1315.1	The fabrication method is complex, expensive, and involves multiple steps, making scalability challenging.	ACS Appl. Nano Mater. 2024, 7(14), 16475-16487.
ZnO/MWCNTs	CNT composite	Arc discharge	Vapor	15.2	Energy-intensive synthesis and very low iodine uptake.	Sci. Rep., 2024, 14, 4242
CCNL carbon dots	Carbon dots	Hydrothermal + multistep assembly	Vapor	231.9	Complex synthesis and limited structural tenability.	Chem. Eng. J., 2024, 479, 147753
Ag@ACF	Activated carbon fiber composite	Hydrothermal functionalization	Vapor	372	Improved porosity but limited chemisorption capability.	Appl. Surf. Sci., 2024, 643, 158644
Coconut shell activated carbon	Carbon	Carbonization/activation	Vapor	790	Although the carbon system is simple, it lacks sufficient functional adsorption sites.	Chem. Eng. J., 2024, 489, 151423
NS-POPs (N,S-containing POPs)	Porous organic polymer	Schiff-base condensation	Vapor / cyclohexane	5100-5430 / 504.4-664.6	Nitrogen, sulfur, and π-conjugated electron-rich frameworks promote strong iodine binding, although the materials require multistep polymer	ACS Appl. Polym. Mater., 2024, 6, 7478–7487

					synthesis and extended reaction times.	
CNT / NCNT / OCNT	CNT	CVD / oxidation / calcination	Vapor	28.9-60.9	Surface modification improves uptake but remains low; adsorption in limited media.	Appl. Surf. Sci., 2023, 629, 157387
Walnut shell activated carbon	Carbon	High-temperature pyrolysis	Vapor	606	High-temperature synthesis; moderate iodine uptake.	Chem. Eng. J., 2023, 454, 140365
Bi-rGO	Graphene composite	Solvothermal reduction	Vapor	1228	Metal incorporation improves iodine affinity in graphene framework.	ACS Appl. Mater. Interfaces, 2023, 15, 40438–40450
Sdots	Sulfur quantum dots	Solvothermal (S + oleylamine, 180 °C)	Vapor/ cyclohexane	2676 / 290	A facile synthesis method enables hydrophobic Sdots to achieve ultrahigh iodine uptake through the synergistic effects of sulfur- and nitrogen-rich sites along with the hydrophobic surface.	This work